e-ISSN: 2548-060X

International Journal of Energy Applications and Technologies

journal homepage: www.dergipark.gov.tr/ijeat

Original Research Article

Numerical simulation of flow over NACA 0015 airfoil with different turbulence models

Neslihan Aydın[1*], Mehmet Erman Çalışkan[1], İrfan Karagöz[1]

[1] *Department of Mechanical Engineering, Uludag University, 16059, Bursa, Turkey*

ARTICLE INFO

* Corresponding author
nslhngunes@uludag.edu.tr

Received February 21, 2020
Accepted May 10, 2020

Published by Editorial Board Members of IJEAT

doi: 10.31593/ijeat.692291

ABSTRACT

Airfoils in various types are widely used in many devices subjected to fluid flows such as aircrafts, vehicles, turbines etc. Therefore, analyzing the fluid flow around an airfoil is one of the important subjects in fluid mechanics. In this study, the conservation equations of two dimensional compressible flow over standard airfoils were solved by using different numerical techniques. After a mesh independence study, applied mathematical model, numerical techniques and obtained results are confirmed with experimental results given in literature. Three different turbulence models, namely the k-w spalarat almaras and the reynolds stress models were used in the solutions. The performances of turbulence models were evaluated under the results obtained. The verified numerical model was also applied to the flow over different types of blades, including a special airfoil design. Velocity and pressure fields obtained around these airfoils were analyzed, and their aerodynamic performances in terms of the lift and drag coefficients were compared to each other at different angles of attack.

Keywords: Renewable energy; Computational fluid dynamics; Airfoils; Turbulence models; Lift and drag coefficients

1. Introduction

Energy is indispensable for us human beings. Alternative methods can be used to obtain energy from renewable energy. Some of these methods are solar energy, wind energy and hydroelectric energy. One of the most widely used renewable energy types is wind energy. This energy type is generally obtained as electrical energy from wind turbines. One of the parts to be considered in the design of the turbine are blades. The air flow around the turbine blades affects the amount of electric current generated. Therefore, the velocity of the air flow around the airfoil design and the variation of the airfoil profile shapes have been investigated many researchers.

Recently, flow phenomena passing through solids have been an important research subject due to aerodynamic effects such as lifting and drag on solid bodies. Especially in airfoil design, different shape airfoil profiles and their aerodynamic effects have been an important research subject.

Başak & Demirhan (2017) proposed a study, were inspired by the fins of the humpback whales and they developed tubercled airfoil design. As a result, they found that the tubercled airfoil compared to normal airfoil design increased efficiency by approximately 42.09 % at the speed of 100 m/s [1]. An experimental and numerical study by a researcher's goals to study the flow around NACA 0015 airfoil design every 2º angles of attack ranges from 2 to 18 º. Numerical analysis results were studied Computational Fluid Dynamics with different turbulences models: the Spalart Allmaras and the k-epsilon. They found that the best results for lift and drag coefficient were obtained 16º attack angle [2]. A numerical simulation aimed to study and analyzing the aerodynamic characteristics of NACA0012 airfoil was carried out by a scholar, the study focused on the designing a airfoil with better aerodynamic performance. NACA 0012 tested with the Large Eddy Simulation Model and the turbulence flow structure in detail for different attack angles by CFD analysis [3]. The flow behavior over AG-16 airfoil was studied and analyzed numerically by researchers, aerodynamic performance for AG-16 airfoil at different angles of attack ranging from 0 degree to 15 degrees was performed, the numerical solution was obtained using ANSYS-FLUENT program. They found that the maximum lift coefficient for high lift airfoil type AG-16 recorded at 0.0116 and the drag coefficient magnitude was equal to 0.0013 when the angle of attack reached the stall limit [4]. A numerical study was analyzed with k-ω shear stress transport model (SST Model) turbulence intensities 1% and 5% predict to velocity inlet and pressure outlet validation with NASA Langley Research Center validation cases. NACA 0012 airfoil subjected to different flap angles and Mach number. They calculated lift coefficients (C_L), drag coefficients (C_D) and C_L/C_D ratio at different operating conditions and showed that with increasing Mach number (M) C_L increases but C_D remains somewhat constant [5]. Matyushenko et al. investigated numerically and experimentally airfoils with different shapes and thicknesses at high Reynolds numbers ($Re \geq 10^6$) and low turbulence intensity ($I \leq 0.1\%$) using two-dimensional Reynolds-Averaged Navier-Stokes equations (RANS) closed by different turbulence models. Results show that comparison with the corresponding data for the γ-SST model; both models are unable to predict the dependence of the lift coefficient on the angle of attack [6]. Holden et al. investigated the design of wind turbine blade that inspired by maple seed in their study. As a result of the study biomimetic wind turbine airfoil maple seed profile Cp power coefficient increased to a maximum value of 0.59 when they calculated CFD results. They also reached C_L value up to 0.8 for maximum Re=10000 [7]. In this study, unlike other studies in the literature, the effect of different turbulence models on aerodynamic structure over the airfoil was examined.

2. Turbulence Models

In order to examine the velocity and pressure distributions in a flow field, the conservation of mass and momentum equations must be solved under the existing boundary conditions [8]. However, it is difficult and even impossible to define these conservation equations in complex geometries and solve them analytically. Therefore, equations must be solved numerically.

The motion of a viscous fluid conforming to Newton's law Navier-Stokes equations is defined as differential with. Navier-Stokes equations, control volume of fluid is formulized the differential form of conservation of momentum [9]. Navier-Stokes equations in Cartesian coordinates are expressible as follows;

$$x - direction = u\frac{\partial u}{\partial x} + v\frac{\partial u}{\partial y} + w\frac{\partial u}{\partial z} = -\frac{1}{P}\frac{\partial P}{\partial x} + g_x + v\left(\frac{\partial^2 u}{\partial x^2} + \frac{\partial^2 u}{\partial y^2} + \frac{\partial^2 u}{\partial z^2}\right) \quad (1)$$

$$y - direction = u\frac{\partial v}{\partial x} + v\frac{\partial v}{\partial y} + w\frac{\partial v}{\partial z} = -\frac{1}{P}\frac{\partial P}{\partial y} + g_y + v\left(\frac{\partial^2 v}{\partial x^2} + \frac{\partial^2 v}{\partial y^2} + \frac{\partial^2 v}{\partial z^2}\right) \quad (2)$$

$$z - direction = u\frac{\partial w}{\partial x} + v\frac{\partial w}{\partial y} + w\frac{\partial w}{\partial z} = -\frac{1}{P}\frac{\partial P}{\partial z} + g_z + v\left(\frac{\partial^2 w}{\partial x^2} + \frac{\partial^2 w}{\partial y^2} + \frac{\partial^2 w}{\partial z^2}\right) \quad (3)$$

Differential continuity equation is based on the principle of conservation of mass in control volume. It is obtained by differential form Cartesian coordinates as follows;

$$\frac{\partial(\rho u)}{\partial x} + \frac{\partial(\rho v)}{\partial y} + \frac{\partial(\rho w)}{\partial z} = 0 \quad (4)$$

By assuming a constant density in equations (1), (2), (3) and (4); in incompressible flows unknown terms are velocity components and pressure in the x, y and z direction. By solving these four equations, these four unknown value can be obtained. On the other hand, Navier-Stokes equations cannot be solved analytically without any simplification. The flow problem is defined within the numerical solution with boundary and initial value conditions and the result is obtained for each discrete point. However, in order to use the equations that model turbulence with Navier- Stokes equations given in Equation (1), the Navier- Stokes equations need to be optimized. With turbulence models to use Reynolds-Averaged Navier-Stokes (RANS) equations are obtained.

2.1. Reynolds-Averaged Navier- Stokes equations RANS

In these equations, flow properties are separated time-averaged and time-varying parts. It is divided into two components. Other values, such as pressure, are expressed as components, such as velocity values. The Navier-Stokes equations are arranged using this principle and Reynolds Mean Navier-Stokes (RANS) equations are obtained. Time resolved RANS equations Time-Dependent Reynolds Averaged Navier- Stokes (URANS) equations are called. Continuity equation and URANS equations Equation (5) and Equation (6) respectively.

$$\frac{\partial \rho}{\partial t} + \frac{\partial}{\partial x_i}(\rho u_i) = 0 \quad (5)$$

$$\frac{\partial}{\partial t}(\rho u_i) + \frac{\partial}{\partial x_j}(\rho u_i u_j) = -\frac{\partial \rho}{\partial x_i} + \frac{\partial}{\partial x_j}\left[\mu\left(\frac{\partial u_i}{\partial x_j} + \frac{\partial u_j}{\partial x_i} - \frac{2}{3}\delta_{ij}\frac{\partial u_i}{\partial x_j}\right)\right] + \frac{\partial}{\partial x_j}\left(-\rho\overline{u_i' u_j'}\right) \quad (6)$$

Here u_i is velocity components and $\left(-\rho\overline{u_i' u_j'}\right)$ indicates Reynolds turbulence stress. Due to the chaotic nature of turbulence there is no analytical method for calculating these values. Turbulence models are used to calculate the turbulence stresses in the momentum equation. Turbulence models have been developed to calculate these values.

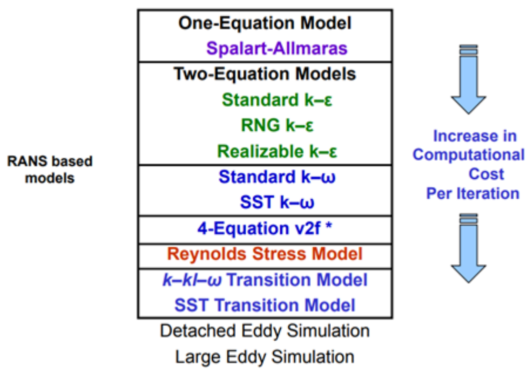

Fig 1. Turbulence models used in ANSYS [10].

2.2. Spalart-Allmaras model

This model is a one equation model for turbulent viscosity and it solves just one transport equation for viscosity; Spalart-Allmaras is a low-cost RANS model solving a transport equation for a modified eddy viscosity. In particular, it gives good results in the flow around the wall in the boundary layer. Turbomachinery has started to gain popularity in applications [11,12].

$$\frac{\partial}{\partial t}(\rho\hat{v}) + \frac{\partial}{\partial x_j}(\rho\hat{v}u_i) = G_v + \frac{1}{\sigma_{\hat{v}}}\left[\frac{\partial}{\partial x_j}\left[\left\{(\mu + \rho\hat{v})\frac{\partial\hat{v}}{\partial x_j}\right\} + C_{b2}\rho\left(\frac{\partial\hat{v}}{\partial x_j}^2\right)\right]\right] - Y_v \quad (7)$$

In equation (7); $\hat{v}$ turbulence kinematic viscosity, G_v turbulence production, Y_v turbulence destruction; $\sigma_{\hat{v}}$ and C_{b2} indicate constants.

2.3. Standard k-ε model

K-ε turbulence model is the most common model used in Computational Fluid Dynamics (CFD) to simulate mean flow characteristics for turbulent flow conditions. It is a two equation model which gives a general description of turbulence by means of two transport equations [13].

The standard k-ε turbulence model; Launder and Spalding, 1974 is used which is based on our best understanding of the relevant processes, therefore minimizing unknowns and presenting a set of equations which can be applied to a large number of turbulent applications [14].

For turbulent kinetic energy (k);

$$\frac{\partial(\rho k)}{\partial t} + \frac{\partial(\rho k u_i)}{\partial x_i} = \frac{\partial}{\partial x_j}\left[\frac{\mu_t}{\sigma_k}\frac{\sigma_k}{\partial x_j}\right] + 2\mu_t E_{ij}E_{ij} - \rho\epsilon \quad (8)$$

For dissipation (**ε**);

$$\varepsilon = v\,\overline{\frac{u_i'}{\partial x_k}\frac{u_i'}{\partial x_k}} \quad (9)$$

Where; ui represents velocity component in corresponding direction, Eij represents component of rate of deformation, μij represents eddy viscosity.

2.4. Standard k- ω model (WİLCOX model)

The other common and simplest model is k-ω model. It provides better modeling of the turbulent boundary layer than the standard k-ε model, however is more sensitive to the free-stream turbulence levels [15]. Given the processes of convection, diffusion and destruction or dissipation, the model equation for ω is given below:

$$\rho\frac{\partial\omega}{\partial t} + \rho U_j\frac{\partial\omega}{\partial x_j} = \frac{\partial}{\partial x_j}\left((\mu + \sigma\mu_t)\frac{\partial\omega}{\partial x_j}\right) + P_\omega - D_\omega \quad (10)$$

The model attempts to predict turbulence by two partial differential equations for two variables, k and ω, with the first variable being the turbulence kinetic energy (k) while the second (ω) is the specific rate of dissipation of the turbulence kinetic energy (k).

$$P_\omega = \alpha\frac{\omega}{k}\tau_{ij}\frac{\partial U_i}{\partial x_j} = \alpha\frac{\omega}{k}P_k \quad (11)$$

$$D_\omega = \beta\rho\omega^2 \quad (12)$$

2.5. Reynolds stress equation model (RSM)

Reynolds stress equation model (RSM), also known as second order or second moment closure model is the nearly most complex classical turbulence model. Several shortcomings of k-ε turbulence model were observed when it was attempted to predict flows with complex strain fields or substantial body forces. Calculation time is longer than other turbulence models, but keep in sight the lack of isotropic turbulence. The Reynolds averaged momentum equations for the mean velocities are:

$$\frac{\partial U_i}{\partial t} + \frac{\partial(\rho u_i u_j)}{\partial x_j} - \frac{\partial}{\partial x_j}\left[\mu\left(\frac{\partial U_i}{\partial x_t} + \frac{\partial U_j}{\partial x_i}\right)\right] = -\frac{\partial p''}{\partial x_i} - \frac{\partial(\rho\overline{u_i u_j})}{\partial x_j} + S_{M_i} \quad (13)$$

Where p'' is a modified pressure, $S_{M_i}$is the sum of body forces and the fluctuating Reynolds stress contribution is $-\rho\overline{u_j u_l}$.

RSM needs more modelling. It is more difficult to convergence. Strong streamline curves are suitable for complex 3D streams with swirl and rotation.

3. Geometry and Mesh Design Parameters

3.1. Geometry design

Naca 0015 airfoil profile that shown in Fig. 2. was used in the analysis. This profile's data files were taken from airfoiltools.com and geometry was designed on Solidworks 2018 as a 3d.

Fig. 2. NACA0015 airfoil

For dimensions of Naca 0015 profile, Robert E. and friend's (1981) paper was used for reasonable compare. Dimension of Naca 0015 airfoil that used in this paper were shown in Fig. 3.

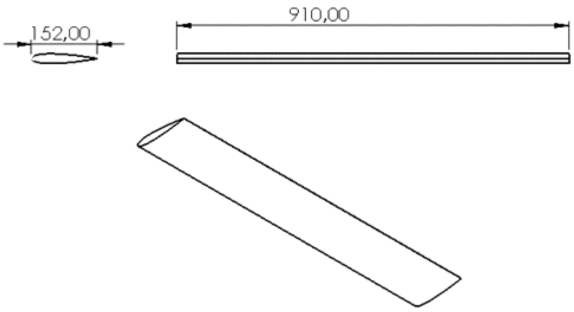

Fig. 3. Dimensions of NACA0015 airfoil profile (units are mm)

A computational flow domain must be covered this Naca 0015 airfoil profile. There are many flow domain types that used in numerical analysis.

In this study, C type geometry was used as a flow domain (Fig. 4.). Because C type mesh structure allows to create less mesh. Also, C type domain is more convenient to create a real flow area [17].

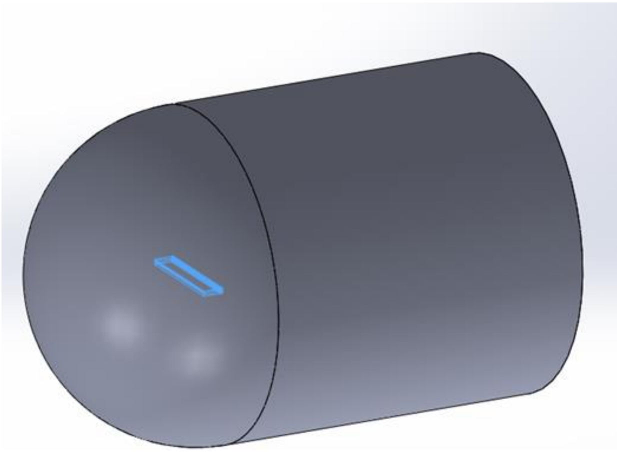

Fig. 4. C type geometry that was designed

In literature, it is suggested that 10x chord length between air inlet and center of profile, and 20x chord length between air outlet and center of airfoil profile (Fig. 5.) [17,18].

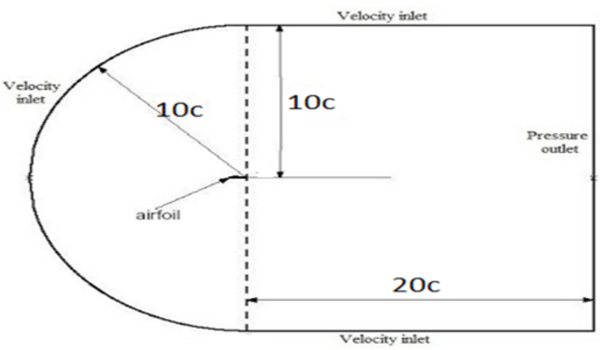

Fig. 5. Certain distances about the C type geometry [18]

Flow domain was subdivided into a series of region. The purpose of this structure is to create appropriately sized mesh in different regions. Thus, it was able to create finer meshes around the airfoil. The regions on geometry are shown in Fig.6.

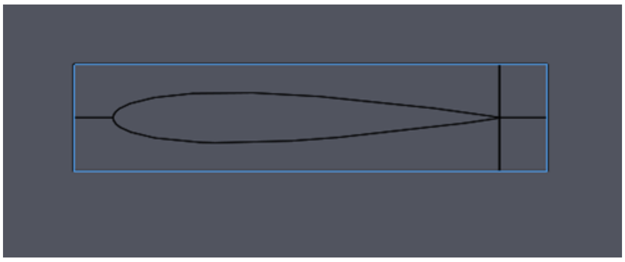

Fig. 6. Different regions on flow domain geometry

3.2. Mesh generation

Mesh generation was made on HYPERMESH 13.0. In order to ensure the desired mesh thickness around the airfoil, different sized mesh elements were generated in different parts of the flow domain geometry. This is done to keep the magnitude of Y-plus as small as possible. The regions in small cells were shown in Fig. 7.

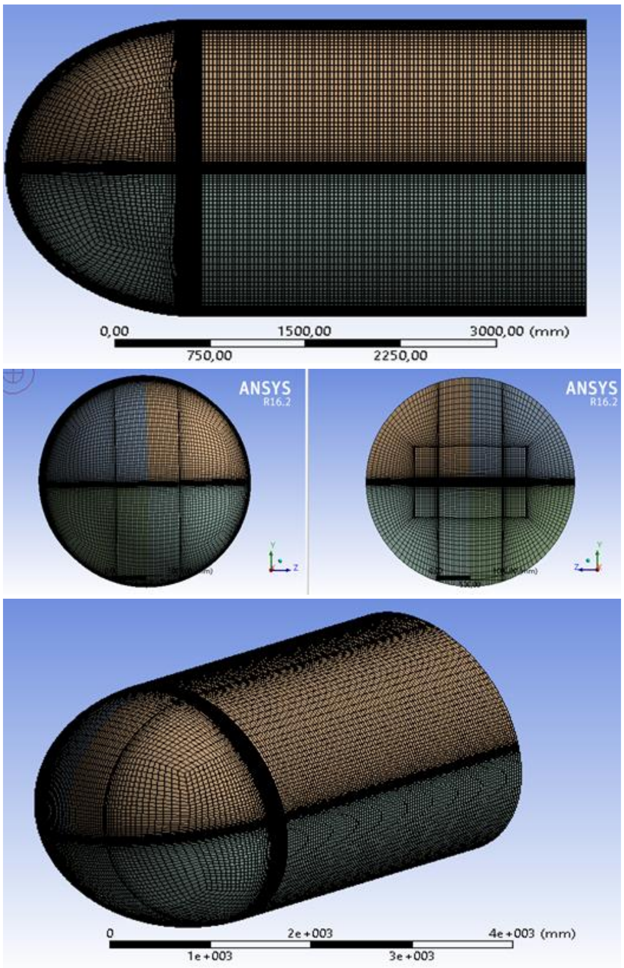

Fig. 7. Different views of mesh elements

Also, fine mesh structure around the airfoil is seen in Fig. 8. in detail. This view was created by middle section of flow domain.

The flow domain is formed by hexa mesh structure. This mesh structure's number of elements is 9533632 and number of nodes 10059476 (Fig. 9.). When creating this mesh structure, 2d mesh structure was created. 3d mesh structure was then generated by these 2d mesh structure.

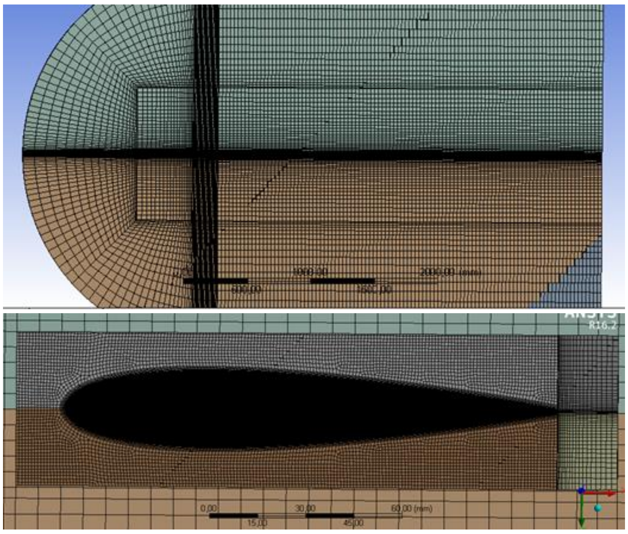

Fig. 8. Section view of mesh elements

Statistics	
Nodes	10059476
Elements	9533632
Mesh Metric	None

Fig. 9. Number of nodes and elements of mesh

3.3. Set up of analysis

For numerical analysis of Naca 0015 airfoil, ANSYS 16.2 and 17.1 fluent was used. During the analysis, the effect of several parameters on the lift and drag coefficient of this airfoil was examined.

For this, certain setups have been made on the program. For solution type, Pressure-Based and Steady Type have been used in the analysis.

The inlet of air was adjusted as shown in the Fig. 5. Magnitude of air inlet velocity, was determined to make the number of Reynolds 40000. So magnitude of inlet velocity was determined as a 4.71m/s.

The attack angles were also adjusted in this section to examine the performance of the airfoil at certain attack angles (Fig. 10.).

Determined values for the reference values were shown in Fig. 11. Area value from these values, was calculated by multiplying the chord length with the airfoil z length (0.152*0.91). The length value was taken as the chord length of 0.152 m.

For solution method, Simple scheme was used. Also other values were given in Fig. 12. in detail.

For Cd (drag coefficient) and Cl (lift coefficient) calculation, certain angle values must be written on the x and y component locations on monitors section in program. How these angle values were calculated was shown in the Fig. 13. and Fig. 14.

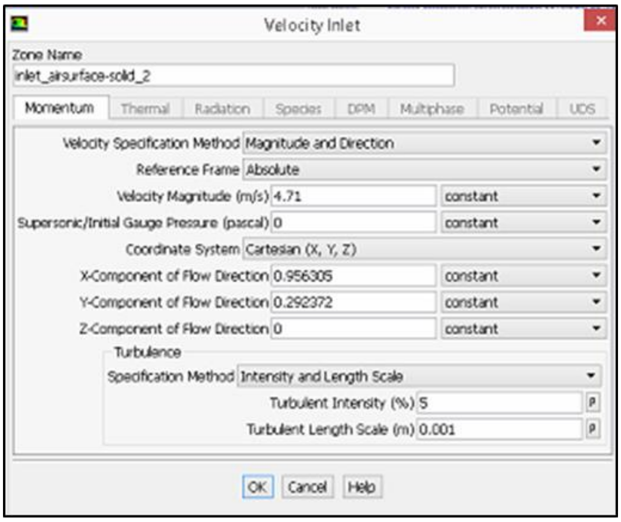

Fig. 10. Setup of the velocity inlet

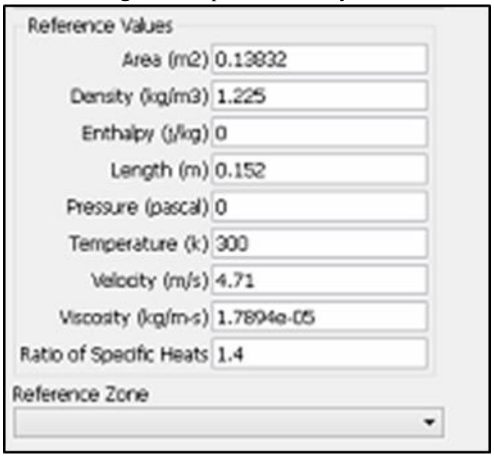

Fig. 11. Reference values

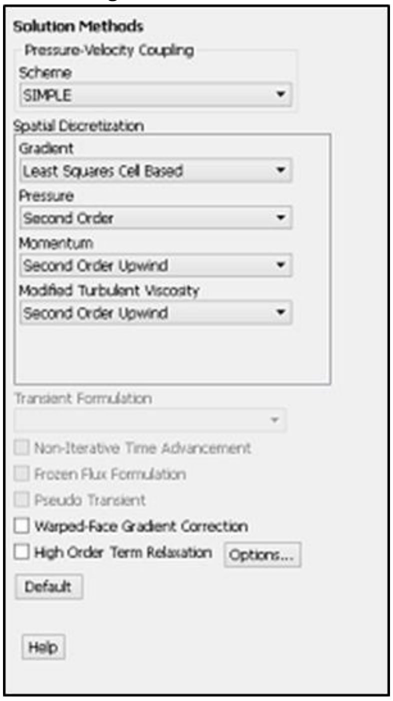

Fig. 12. Setup of solution method

As shown in the Fig. 14., direction must be normal to flow or perpendicular to drag. So mainstream velocity vector must be stated by 90°.

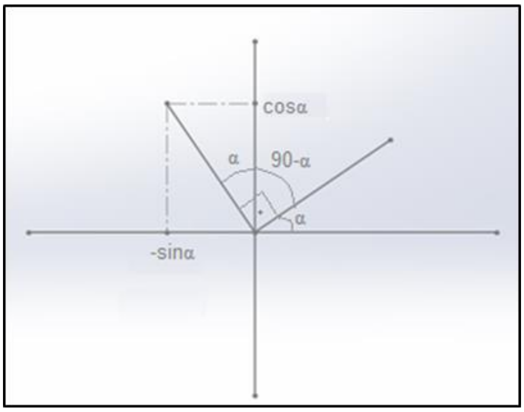

Fig. 13. Vectors of Cl components; calculation of Cl

As shown in the Fig. 14., direction must be same as flow, aligned with chord line or attack angle.

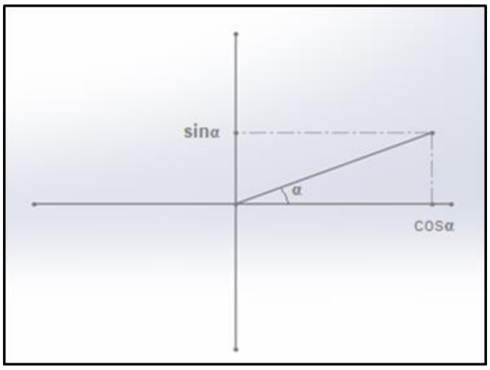

Fig. 14. Vectors of Cd components calculation of Cd

4. Results

In the analysis, firstly, the Cl and Cd coefficients of the Naca 0015 airfoil were examined, with 7° attach angle and 40000 Re number, depending on different turbulence models. These results were compared with the experimental data set in the study of Robert E. and friend's (1981) and turbulence model which gives the best results was determined (Table 1.).

Table 1. Comparison of Cl and Cd coefficients according to turbulence models at 7° attack angle and 40000 Re number

	TURBULENCE MODEL	Cl	Cd
1	Spalart Almaras	0.48543	0.038633
2	k-ε (Realizable)	0.43315	0.053946
3	k-ω (SST)	0.46362	0.037405
4	k-ω (Standart)	0.46825	0.037019
5	Reynolds Stress Model	2.1296	-7.1944
	Experimental Data	0.5730	0.0267

As can be seen from the Table 1, Spalart Almaras model is the most suitable model for experimental data. The Spalart Almaras model best fit for this Naca profile. Reynolds Stress Model is not suitable because of small Reynolds numbers. RSS model will give appropriate results when higher reynolds numbers are tried.

The results obtained from the Spalart Almaras model, with 7° attack angle and 40000 Re number, were examined.

4.1. Scaled residuals

As can be seen from Fig.15., convergence curves are sufficiently reduced.

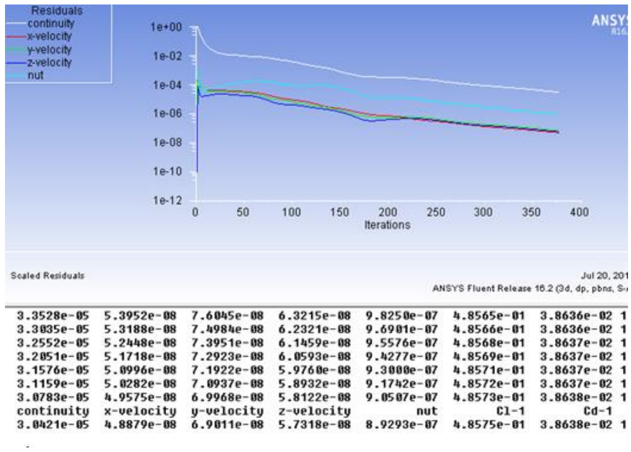

Fig. 15. Scaled residuals of number 1 analysis

4.2. Yplus values

Yplus value is often used to describe how coarse or fine a mesh is for a particular flow pattern. In the airfoil analysis, Yplus value should be examined on the airfoil. Usually this Yplus value is required max value 1. Therefore, the mesh thickness around the airfoil, which is shown in detail in the Fig. 8, was reduced to 0.05 mm.

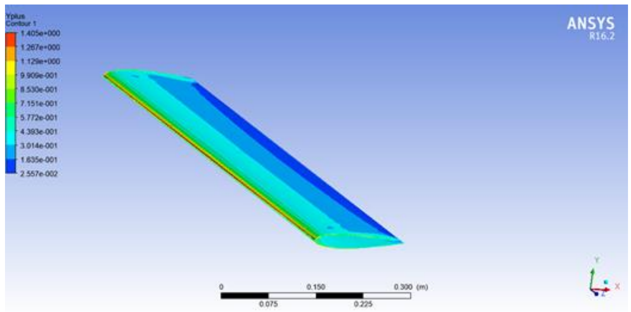

Fig. 16. Y plus values of number 1 analysis

As can be seen from the Fig.16., the max y plus value on the airfoil was obtained from the analysis is 1.405.

4.3. Pressure contours

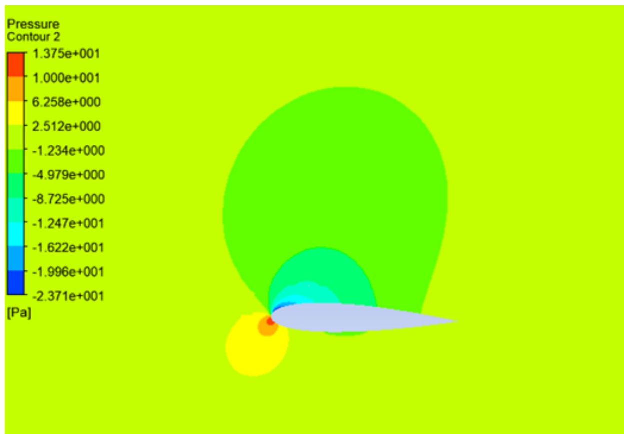

Fig. 17. Pressure contour of number 1 analysis

The high pressure at the bottom inlet of the airfoil has increased up to 13.75Pa. In the upper part of the airfoil, because of the high velocity, the pressure has dropped to -23.71Pa. When the pressure contours are examined, it is seen that the pressure distribution around the airfoil develops regularly.

4.4. Velocity contours

As can be seen in the Fig.18, a wake region was formed in the part where the air is separated from the airfoil. This wake area was about 1 meter long. Air flowed slightly slower than the inlet velocity in the wake region.

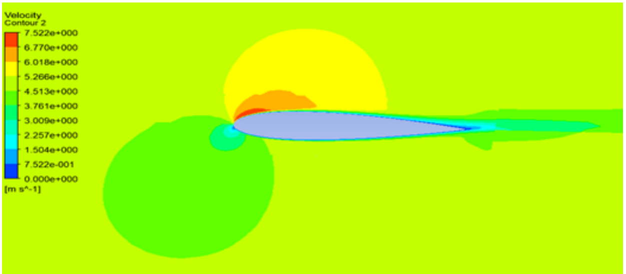

Fig. 18. Velocity contour of number 1 analysis

4.5. Velocity vectors

When air velocity vectors are considered, it is seen that air velocity increases up to 7.52 m/s in upper parts of airfoil after entering air.

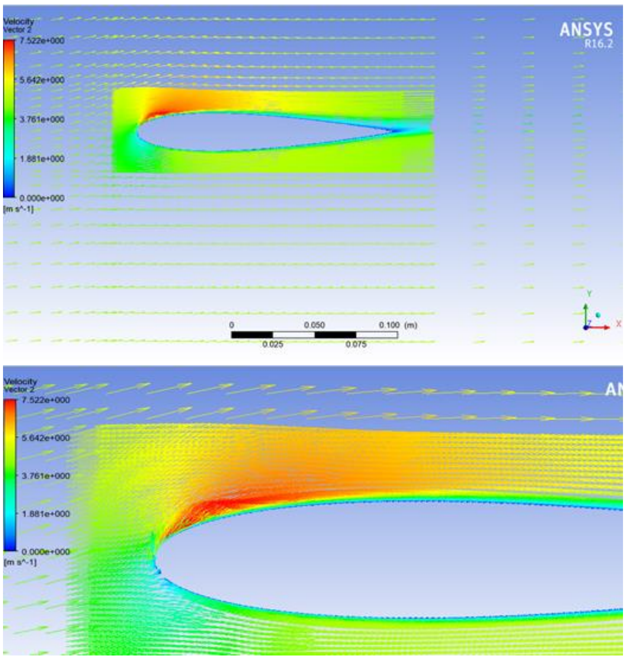

Fig. 19. Velocity vector of number 1 analysis

4.5. Investigation of NACA 0015 airfoil performance according to attack angle

After determining the most suitable turbulence model, C_L and C_D coefficients were examined according to attack angle with 40000 Re number. The results obtained from these analyses between 5° and 18° attack angles are presented in the Fig.20 and Table 2.

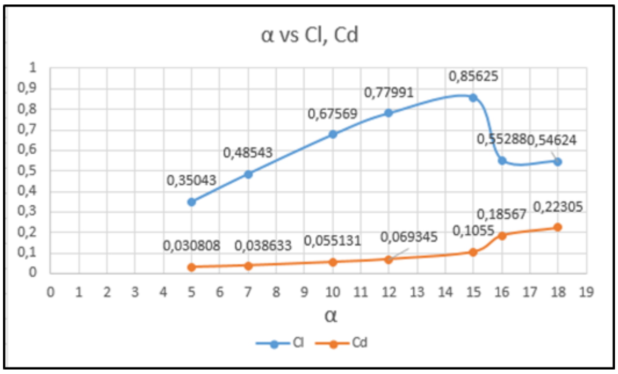

Fig. 20. C_L and C_d values of Naca0015 Airfoil according to attack angle with 40000 Re number

Table 2. CL and CD values of NACA 0015 airfoil according to attack angle with 40000 Re number

α	Cl	Cd	Cl/Cd
5	0.35043	0.030808	11.37464
7	0.48543	0.038633	12.56516
10	0.67569	0.055131	12.25608
12	0.77991	0.069345	11.24681
15	0.85625	0.1055	8.116114
16	0.55288	0.18567	2.977756
18	0.54624	0.22305	2.448958

There is a stall angle where the coefficient of C_L starts to decrease while the angle of attack increases. As can be seen from the Fig.20, this stall angle is 15° for this analysis. Also, the highest ratio of C_L/C_D was observed at 7°.

5. Conclusions

In this paper, NACA0015 Airfoil are investigated with different turbulence methods; k-ε, k-ω, RSM methods.

- C_L and C_D obtained best accuracy with experimental results Spalart-Allmaras method. This model is generally recommended for flow analysis over the airfoil [2].
- In addition, k-w models have been shown to provide good results for flow analysis over the airfoil.
- It was found that Reynolds Stress Model is not suitable for flow analysis. RSM should generally be used in analyzes involving rotating flow
- C_D value increased with attack angle but C_L value was initially increasing with attack angle after a stagnation point these was called as a stall angle or stall point C_L decreased critically. In this study stall angle was 15°.
- The performance of any airfoil is measurement with the C_L/C_D ratio. The highest ratio of C_L/C_D was observed at 7°.
- Therefore, different turbulence models have been analyzed at 7 ° of attack angle.

The max y plus value on the airfoil was obtained from the analysis 1.405. Considering that the max y-plus value should be 1, this result was considered acceptable [17,18].

ORCID
Neslihan Aydın 0000-0003-3650-0886
M. Erman Çalışkan 0000-0002-6123-9627
İrfan Karagöz 0000-0002-7442-2746

References

[1] H. Başak , H. Demirhan , Examination of Airfoil Profile Yield Inspired by The Fins of Humpback Whale with CFD Analysis , Journal of Gazi Engineering Sciences, 2017, 3(2):15-20.
[2] I. Şahin, A. Acir, Numerical and Experimental Investigation of Lift and Drag Performances of NACA0015 Wind Turbine Airfoil, IJMMM 2015 Vol.3(1): 22-25 ISSN: 1793-8198.
[3] L.B. Streher,, "Large-eddy simulations of the flow around a NACA0012 airfoil at different angles of attack",Physics, Fluid Dynamics thesis, Helmut-Schmidt-Universitat der Bundeswehr, Hamburg, May 2017.
[4] A. H. Mutaib, A. AL-Khateeb, M. K. Khashan, F. Kamil, Computational Study of Flow Characteristics Over High Lift Airfoil at Various Angles of Attack, Journal of Mechanical Engineering Research & Developments (JMERD) 42(1) (2019) 90-9.
[5] T. Ahmed, Md. T. Amin, S.M. R. Islam, S. Ahmed, Computational Study of Flow Around a NACA 0012 Airfoil Flapped at Different Flap Angles with Varying Mach Numbers, Global Journal of Researches in Engineering General Engineering Vol.13(4)(2013):5-16.
[6] A. A. Matyushenko, E. V. Kotov, A. V. Garbaruk, Calculations of Flow Around Airfoils Using Two Dimensional RANS: An Analysis of the Reduction in Accuracy,St. Petersburg Polytechnical University Journal: Physics and Mathematics Vol.3(4) (2017):15-21.
[7] J. Holden, T. M. Caley, M. G. Turner, Maple Seed Performance as a Wind Turbine, Conference: AIAA SciTech 2015, At Kissimmee, FL, Volume: AIAA 2015-1304. DOI: 10.2514/6.2015-1304.
[8] Y. A. Çengel, J. M. Cimbala, Solutions Manual for Fluid Mechanics: Fundamentals and Applications Second Edition, McGraw-Hill, 2010.
[9] B. Apaçoğlu, "Cfd Analyses of Uncontrolled and Controlled Laminar and Turbulent Flows Over A Circular Cylinder", Mechanical Engineering Master thesis, TOBB University of Economics and Technology, Ankara 2010.
[10] ANSYS FLUENT 13.0 Lecture 06 Turbulence User Guide,2013.
[11] P.R.Spalart, S.R. Almaras, A One-Equation Turbulence Model for Aerodynamic Flows. 1992. AIAA Paper 92-0439.
[12] H. B. Ekmekci, "Modification Of A Computational Fluid Dynamics Model (Ansys-Fluent) For The Purpose Of River Flow And Sediment Transport Modeling", Master of Science in Civil Engineering Thesis, The Graduate School of Engineering and Sciences of İzmir Institute of Technology, İzmir, July, 2015.
[13] F.Kaya, İ. Karagöz, Investigation into the Suitability of Turbulence Models in Swirling Flows, Uludag University Journal of The Faculty of Engineering Vol 12(1) (2007):85-96.
[14] B.E. Launder, D.B. Spalding, The Numerical Computation of Turbulent Flows. Computer Methods in Applied Mechanics and Engineering, 3, (1974) 269-289.
[15] D.C. Wilcox, Turbulence Modeling for CFD. 2006, DCW Industries, Inc.
[16] R. E Sheldahl, P. C. Klimas, Aerodynamic characteristics of seven symmetrical airfoil sections through 180-degree angle of attack for use in aerodynamic analysis of vertical axis wind turbines (No. SAND-80-2114). Sandia National Labs., Albuquerque, NM (USA). (1981).
[17] Y. Khichine, M. Sriti, Boundary Layer and Mesh Refinement on Aerodynamic Performances of Horizontal Axis Wind Turbine (HAWT), International Journal of Mechanical Engineering Vol 2 (2017):119-125.
[18] D. C. Eleni, T. I. Athanasios, M. P. Dionissios, Evaluation of the Turbulence Models for the Simulation of the Flow over a National Advisory Committee for Aeronautics (NACA) 0012 Airfoils, Journal of Mechanical Engineering Research Vol. 4(3), pp. 100-111, March 2012.